

Journal of Biomedical Optics

SPIEDigitalLibrary.org/jbo

Impact of contralateral and ipsilateral reference tissue selection on self-referencing differential spectroscopy for breast cancer detection

Anais Leproux
Albert E. Cerussi
Wendy Tanamai
Amanda F. Durkin
Montana Compton
Enrico Gratton
Bruce J. Tromberg

Impact of contralateral and ipsilateral reference tissue selection on self-referencing differential spectroscopy for breast cancer detection

Anaïs Leproux,^a Albert E. Cerussi,^a Wendy Tanamai,^a Amanda F. Durkin,^a Montana Compton,^a Enrico Gratton,^b and Bruce J. Tromberg^a

^aUniversity of California, Irvine, Beckman Laser Institute, 1002 Health Sciences Road, Irvine, California 92612

^bUniversity of California, Irvine, Laboratory for Fluorescence Dynamics, Irvine, California 92612

Abstract. We previously developed a self-referencing differential spectroscopic (SRDS) method to detect lesions by identifying a spectroscopic biomarker of breast cancer, i.e., the specific tumor component (STC). The SRDS method is based on the assumption of the exclusive presence of this spectroscopic biomarker in malignant disease. Although clinical results using this method have already been published, the dependence of the STC spectra on the choice of reference tissue has not yet been addressed. In this study, we explore the impact of the selection of the reference region size and location on the STC spectrum in 10 subjects with malignant breast tumors. Referencing from both contralateral and ipsilateral sides was performed. Regardless of the referencing, we are able to obtain consistent high contrast images of malignant lesions using the STC with less than 13% deviation. These results suggest that the STC measurements are independent of any type, location, and amount of normal breast tissue used for referencing. This confirms the initial assumption of the SRDS analysis, that there are specific tumor components in cancer that do not exist in normal tissue. This also indicates that bilateral measurements are not required for lesion identification using the STC method. © 2011 Society of Photo-Optical Instrumentation Engineers (SPIE). [DOI: 10.1117/1.3652711]

Keywords: near-infrared spectroscopy; diffuse optical spectroscopy; diffuse optical imaging; multiple light scattering; cancer imaging.

Paper 11321R received Jun. 24, 2011; revised manuscript received Sep. 21, 2011; accepted for publication Sep. 23, 2011; published online Nov. 2, 2011.

1 Introduction

Diffuse optical spectroscopy (DOS) and imaging (DOI) are techniques designed to measure functional and structural information content from deep below tissue surfaces. Various forms of DOS and DOI, which employ near-infrared (NIR) light, have been used extensively in breast cancer research. Disease detection and localization are enabled by strong endogenous optical property contrast (i.e., absorption and scattering) between tumors and normal breast tissue.^{1–5} Multispectral approaches and model-based methods that account for tissue scattering are used to quantitatively measure the tissue concentration of hemoglobin (oxygenated and deoxygenated) and other chromophores such as lipid and water. Increased hemoglobin and water concentration in tumors relative to normal breast tissue has been widely observed in the literature. These changes are understood to be a direct result of tumor physiology, including angiogenesis, cellular proliferation, and edema.^{2,3,6–8}

Promising results characterizing concentration differences between tumors and normal tissue for the four main breast chromophores (deoxy-hemoglobin, oxy-hemoglobin, water, and lipid) have been shown using DOS and DOI.^{9–11} However, these components are not unique to malignant tumors. Normal physiological features may thus obscure the presence of malignancies, limiting lesion detection and differential diagnosis (i.e., distinguishing between malignant and benign tumors). For this reason,

we have investigated the use of high spectral bandwidth DOS approaches to characterize spectral shifts in tissue absorption features that reflect changes in the presence or disposition of intrinsic tissue components.

Using this approach in pilot clinical studies we recently reported that NIR absorption spectra from invasive breast cancers have a “specific tumor component” (STC) that appears to be absent from normal tissues, and is distinctive from benign tumors.^{12,13} The STC is detected using a self-referencing differential spectroscopic (SRDS) method that extracts subtle spectral shifts between reference and sample tissue volumes. The STC is determined by taking the difference between sample and reference tissue absorption spectra (first differential) and obtaining the residuals of the fit of this first differential to the four-component basis chromophores of breast tissue. In this approach, spectral components not accounted for in the basis spectra that differ between sample and reference tissues are the only components in the residuals. Importantly, the typically high interpatient biological variations in normal tissues are canceled because for each patient, the data are referenced to their own unique spectral-molecular profile.

One important question that has not been addressed is the verification of the initial assumption of the SRDS analysis. If the STC component is truly unique to cancer, then we expect that the choice of reference tissue will not significantly impact the detection of the STC spectrum, provided it samples normal tissue. In this paper, the exclusiveness of this imaging biomarker

Address all correspondence to: Bruce Tromberg, Beckman Laser Institute, 1002 Health Sciences Road, Irvine, California 92612. Tel: 9498240255; E-mail: bjtrombe@uci.edu.

to malignant tumors was investigated by studying the influence of the choice of the reference (i.e., normal) tissue on the spectral shape and spatial distribution of the STC.

We report the results of a 10 patient study that assesses the influence of the number and location of reference measurement points on the STC spectrum of malignant lesions. Both ipsilateral and contralateral tissues were investigated using tissue mapping methods that sampled up to 156 unique spatial locations on each breast with full absorption and scattering spectra (650 to 1000 nm) measured at each spatial location. To account for interpatient variability, we show that the character of the STC images are minimally influenced by the choice of reference tissue sites from contralateral or normal ipsilateral breast. Our results support the idea that SRDS analysis can be used to identify specific tumor components in cancer regardless of the normal tissue reference location. This finding also implies that bilateral measurements are not required for lesion detection using the SRDS technique.

2 Materials and Methods

2.1 Instrument

A description of the basic components of our diffuse optical spectroscopic imaging (DOSI) instrument has been previously presented.^{14,15} Briefly, DOSI consists of a combined frequency-domain photon migration (FDPM) component and a broadband steady-state (SS) component integrated together to produce broadband absorption and scattering spectra of tissues from 650 to 1000 nm. The FDPM component uses 6 laser diodes at the wavelengths 658, 682, 785, 810, 830, and 850 nm. The breast is illuminated sequentially by each laser diode, which is intensity modulated at 401 modulation frequencies swept from 50 to 400 MHz. The backscattered light is detected by an avalanche photodiode mounted inside a hand-held probe. The SS component uses a high-intensity tungsten-halogen source. The backscattered light is detected by a grating-based spectrometer that collects light from 650 to 1000 nm (1024 pixels). The FDPM and SS sources are coupled by optical fibers mounted into the hand-held probe. The source-detector separation was 28 mm for both FDPM and SS components.

FDPM and SS data are combined to provide broadband absorption (μ_a) and reduced scattering (μ_s') spectra from 650 to 1000 nm. Briefly, we start with the FDPM measurement. The phase and amplitude as functions of modulation frequency are fit to a diffusive model of light transport (semi-infinite boundary conditions) to recover μ_a and μ_s' at each of the six laser wavelengths. SS broadband spectra were converted into absolute absorption spectra using two simple steps. First, the spectral shape of the reduced scattering spectrum is assumed to follow a power law of the form $\mu_s' = A\lambda^{-sp}$, where A is the scatter amplitude and sp is the scatter power, or the exponent of the scattering spectrum. The power-law fit to the FDPM discrete laser diode spectrum provides a scatter correction for the SS reflectance spectrum. We then fit the SS reflectance intensity at each of the laser diode wavelengths to the reflectance calculated from the FDPM-measured absolute absorption values. Thus, the SS reflectance spectrum intensity is scaled using the FDPM discrete laser diode measurements. The absolute absorption spectrum is

then extracted by fitting the corrected reflectance spectrum to a diffusion reflectance model.

2.2 Spectral Analysis

Spectral analysis is performed on the absorption data assuming that the absorption in normal breast is caused mainly by the following four chromophores: deoxy-hemoglobin (ctHHb), oxy-hemoglobin (ctO₂Hb), water (ctH₂O), and bulk lipid (ctlipid). We recover these chromophore concentrations by fitting a linear combination of their molecular extinction coefficient spectra to the scatter-corrected absorption spectrum.¹⁰ The STC is determined by taking the difference between sample and reference tissue absorption spectra and analyzing the residuals of the fit of this first differential to the four-component basis chromophores of breast tissue. Details of this SRDS method have been reported.¹²

In order to quantify the STC spectrum, an STC index was defined by the sum of all local residual variances L_k calculated over five specific spectral regions:¹²

$$\text{STCindex} = \sum_{k=1}^5 L_k = \sum_{k=1}^5 \left(\sum_i \text{STC}_i(\lambda_i, x, y)^2 / N_k \right). \quad (1)$$

The local variance L_k is a function of position on the breast given by x and y coordinates. The index k indicates a given spectral region and N_k indicates the total number of wavelengths in the spectral region. $\text{STC}_i(\lambda_i, x, y)$ is the value of the STC spectra at a given wavelength. The spectral regions are as follows: 650 to 665, 730 to 800, 875 to 930, 930 to 960, and 980 to 990 nm. They have been defined empirically to maximize the differences between tumor and normal: systematic differences were found in the STC spectra of tumor as compared to STC spectra of normal breast tissue in these five regions.¹² The biochemical origin of these features are broadly related to hemoglobin, lipid, and water. Then, calculating the STC index for each spatial measurement point of the breast (see below for measurement description), an STC index map can be obtained. As the STC index is based on wavelength regions sensitive to the tumor signature, STC index maps can be used for lesion visualization or detection.

2.3 Patients and Measurement Procedure

Study protocols were approved by the Institutional Review Board of the University of California, Irvine, and written informed consent was obtained from all patients. A total of 11 female breast cancer patients were investigated. Patients were excluded in this study in the case of multiple unilateral lesions, big bilateral lesions, lesions smaller than 10 mm, or a noninvasive form of carcinoma. In addition, only datasets with available data from the contralateral breast, and performed as grid scan (and not line scan) were used in this study.

The patients' information can be found in Table 1. The patients' ages ranged from 31 to 64 years old, with an average age of 50, including 6 premenopausal (pre) and 5 postmenopausal (post) patients. Two patients had bi-lateral lesions; one patient had bi-lateral infiltrating ductal carcinoma (IDC), and the other patient had infiltrating lobular carcinoma (ILC) and sclerosing adenosis in the left and right breasts, respectively. In these two patients, only the lesion in the left breast was investigated. The

Table 1 Patients' characteristics.

Patient nr	Age (year)	Menopausal status	BIRADS	Histology	TNM score	Side	Size at max (mm)
1^a	48	pre	3	IDC	9	Right	18
2	31	pre	4	IDC	8	Right	50
3	56	post	2	IDC	4	Right	14
4^b	63	post	3	IDC	8	Left	29
5	55	post	NA	IDC	7	Left	18
6	61	post	2	IDC	8	Left	90
7^c	37	pre	4	ILC	3	Left	25
8	64	post	2	IDC	6	Left	26
9	43	pre	4	IDC	9	Right	25
10^d	38	pre	NA	IDC	9	Right	42
11^d	49	pre	2	IDC	8	Right	26

NA, not available.

^aLesion not visible in DOSI images.

^bIDC in the right breast.

^cSclectrosing adenosis in the right breast.

^dCystic breasts.

b and c are located outside the field of view of the DOSI measurements.

lesion in the other breast (right breast) was small and was not in the measurement field of view. Therefore, the right breast was referred to as the contralateral normal side for these two patients. Two other patients were reported as having cystic breasts. For the remaining seven patients, the contralateral breasts were mass-free according to the diagnostic imaging reports. The current study included a total of 11 masses; 10 IDC, and 1 ILC. Out of the 11 patients, 3 had a breast density of BIRADS 4 (75% to 100% glandular tissue), 2 had BIRADS 3 (50% to 75% glandular tissue), 4 had BIRADS 2 (25% to 50% glandular tissue), and the remaining 2 patients had unknown breast densities.

DOSI maps from both breasts were collected for each patient. Patient-specific measurement grids to define DOSI measurement locations were chosen based on the lesion size, location, and on the breast size. DOSI measurements were performed over the region of the lesion and over surrounding normal tissue, and in the same location mirrored on the contralateral side. The measurement grids were drawn in 10 mm steps in both x and y directions. The dimension of the measurement grids ranged from 90×40 to 120×130 mm, resulting in up to 156 discrete measurement locations for each breast. The specific details of patient positioning have been recently described.¹⁶

In 1 out of the 11 patients, we were not able to visualize the lesion in the DOSI image. The lesion to background contrast was probably too low to be detected with our scanner. The dataset of this patient was therefore not included in the data analysis.

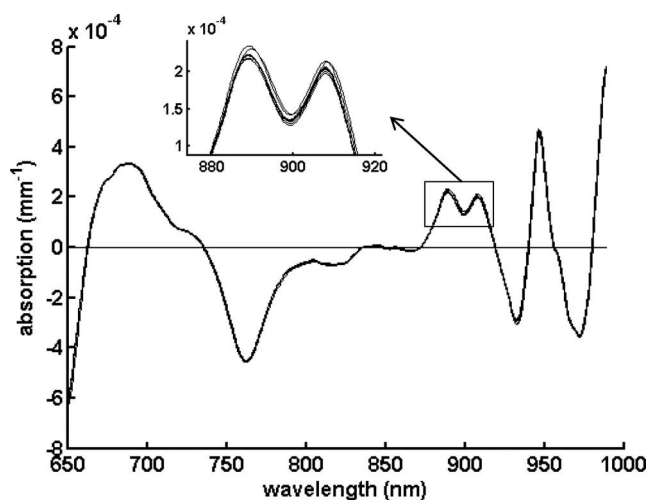
2.4 Data Analysis

The areola was included, partly or entirely, in the field of view of the optical images in 7 out of 10 patients. For data analysis,

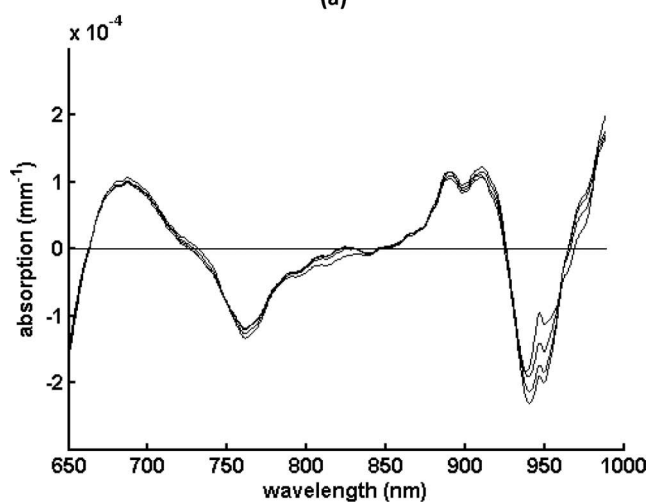
the areolar regions were defined in the optical images based on a previously described contrast function, the tissue optical index ($TOI = ctHHb \times ctH_2O/ctlipid$) and on the size of the areola in the clinical report. The tumor location defined in the optical images was based on the TOI and ultrasound information of the clinical report. The "normal" reference tissue in the ipsilateral breast was defined by excluding the tumor region and an additional ~ 1 cm wide zone around the tumor. Spectral analysis of tumors was performed on the tumor point showing the highest STC value.

2.5 Statistical Analysis

The maps obtained using different referencing techniques were compared for similarity. To compare the equivalence between two methods, one must show that the difference between the data obtained using both methods is small enough to use the methods interchangeably. Statistically, one must reject the null hypothesis, which is the data obtained using both methods are not different, and a confidence interval of the subtracted data should lay within predefined equivalence limits. This range of equivalence is subjective and is defined *a priori* depending on the clinical/scientific context.^{17,18} Here, we want to obtain similar features in the STC index maps such that the lesion is visible in the maps obtained using any referencing method. We estimated that the main features of the map would be preserved with a 20% maximum difference and hence, the clinical diagnosis would not be affected. Using this threshold, we statistically compared the STC index maps by computing the two one-sided test for equivalence (TOST) using R (version 2.13.1).¹⁹



(a)



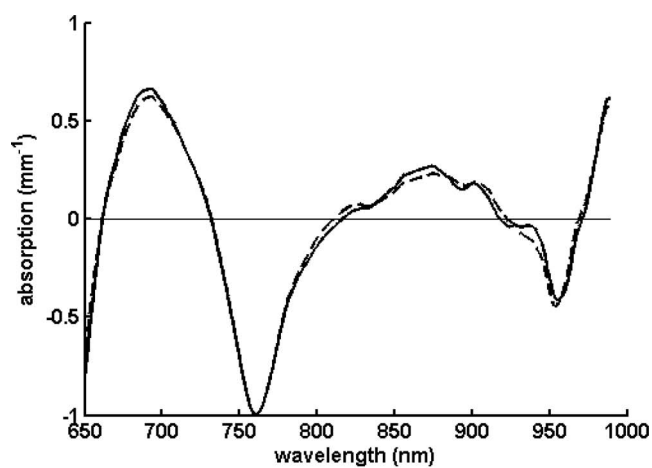
(b)

Fig. 1 Averaged STC spectra calculated using N number of reference locations, where all locations are randomly selected 10 times. (a) Patient 6. $N = 4, 9, 18, 27, 36, 45, 54, 63,$ and 72 . (b) Patient 9: patient with the worst deviations among the results. $N = 6, 9, 20,$ and 30 .

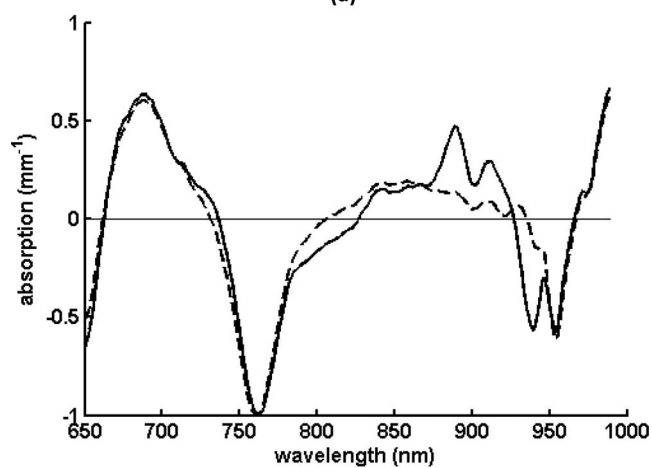
3 Results

3.1 Impact of Amount of Reference Points

Random measurement points across the contralateral side have been selected and used as reference for the calculation of the STC. Fig. 1(a) presents the averaged STC spectra in the lesion of patient 6 calculated successively with 4, 9, 18, 27, 36, 45, 54, 63, and 72 reference locations in the contralateral side. The locations were randomly selected 10 times and the resulting 10 spectra were averaged on the graph. We observe that the spectra overlap closely; 4 reference points produce the same STC spectrum as 72 reference points, i.e., almost the whole contralateral side. This result suggests that only a few measurement points in the contralateral normal breast are required to obtain a reliable STC spectrum. Fig. 1(b) presents the 10 averaged STC spectra in the lesion of patient 9 calculated with successively 6, 9, 20, and 30 random reference points in the contralateral side. In this case, small fluctuations are seen between the spectra: they represent the biggest deviations that were visualized in the 10 patients. For a more quantitative analysis, we compared for all patients



(a)



(b)

Fig. 2 Normalized STC spectra: the solid line is the STC referenced on the ipsilateral side; the dashed line is the STC calculated using the contralateral breast as reference. (a) Patient 10, close STC spectra using the 2 different referencing approaches. (b) Patient 8, different spectral content in part of the spectra.

the averaged STC spectra calculated with $P = 6, 9, 20,$ and 30 reference points, randomly selected 6 times, to the gold-standard STC spectra obtained using the whole contralateral breast. We observed that $P = 6$ reference points results in the largest variance compared to the gold standard with an average correlation coefficient of 0.99 ± 0.01 (range 0.97 to 1.00) for all the patients. For spectra calculated with $P > 9$, the correlation coefficient $r > 0.99 \pm 0.01$ (range 0.97 to 1.00). These small variations in STC have a negligible impact upon the STC index, and subsequently the STC index maps which were found to be statistically equivalent in all patients using the TOST analysis (p -value $\ll 10^{-6}$).

3.2 Impact of Referencing on the Ipsilateral Side

A key question is whether the information contained in the STC is preserved when the selected reference normal tissue shifts from the contralateral to the ipsilateral side. To address this issue, we performed comparisons of STC obtained from the 10 lesions calculated using reference locations on both sides, as shown in Fig. 2. In six patients there were minimal differences

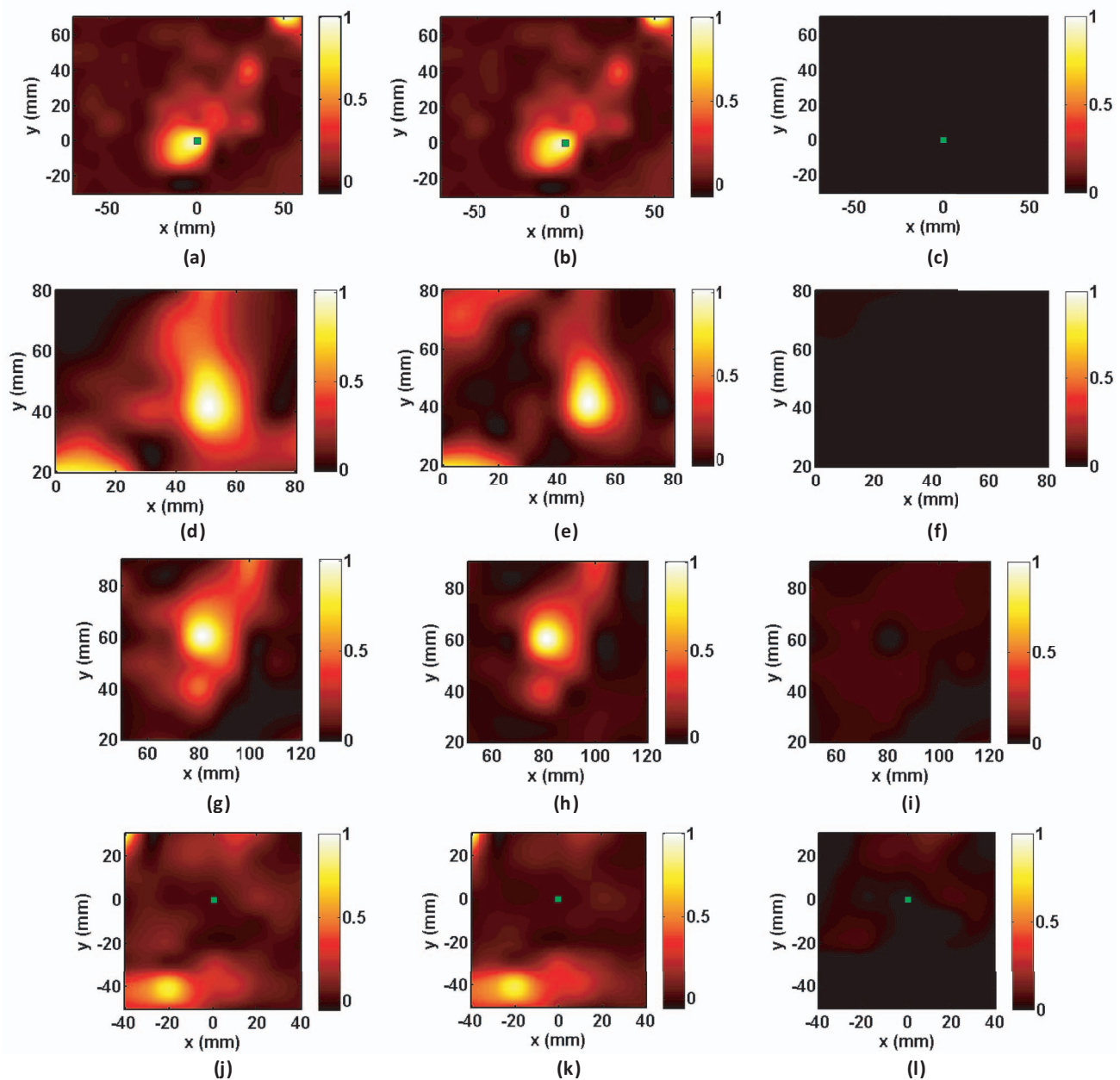


Fig. 3 (a) and (b) STC index maps of patient 2. (c) Subtracted map of patient 2. (d) and (e) STC index maps of patient 5. (f) Subtracted map of patient 5. (g) and (h) STC index maps of patient 8. (i) Subtracted map of patient 8. (j) and (k) STC index maps of patient 9. (l) Subtracted map of patient 9. The STC index maps in (a), (d), (g), and (j) are obtained using the contralateral breast as reference. The STC index maps in (b), (e), (h), and (k) are obtained using the background tissue of the ipsilateral breast as reference.

between STC spectra [i.e., similar to Fig. 2(a)]. We found an average correlation coefficient of 0.98 ± 0.03 (range 0.92 to 1.00) between the spectra referenced on the areola compared with the whole contralateral breast for these six patients. These spectra produced negligible differences in the STC index maps. We found an average mean value of the subtracted maps (i.e., STC with ipsilateral reference versus STC via contralateral reference) of 0.018 (ranging from 0.009 to 0.027) with an average standard deviation (SD) of 0.013 (ranging from 0.007 to 0.023). In the remaining four subjects (Nos. 2, 5, 8, and 9) more noticeable variations were observed between STC spectra [i.e., similar to Fig. 2(b)] calculated with the contralateral breast and the nor-

mal healthy tissue in the ipsilateral breast for the reference. The STC spectra showed different magnitudes or small peak shifts around the spectral region 850 to 950 nm. We found correlation coefficients of 0.75, 0.88, 0.79, and 0.92 between the spectra referenced on the areola compared with the whole contralateral breast for patients 2, 5, 8, and 9, respectively. Fig. 3 presents the normalized STC index maps of these patients calculated with the contralateral breast and the normal healthy tissue in the ipsilateral breast for the reference, and their subtracted maps. Even though the STC spectra of these patients calculated with both referencing showed different spectral content, we observe here that the STC index maps are still similar: the lesion position

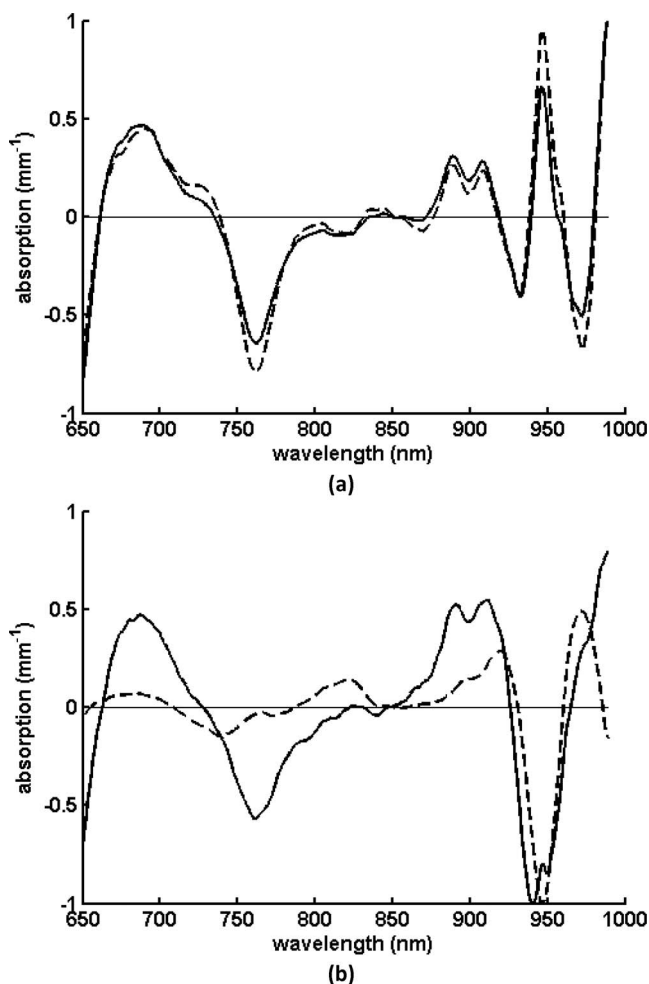


Fig. 4 STC spectra in lesion calculated with reference normal tissue in the whole contralateral side, solid line, and in the areola of the contralateral side, dashed line. (a) Patient 4. (b) Patient 9.

and the main features of the image are preserved, as shown in Fig. 3(a), 3(b), 3(d), 3(e), 3(g), 3(h), 3(j), and 3(k). This result is confirmed by the subtracted normalized maps of the STC index maps in Fig. 3(c), 3(f), 3(i), and 3(l). The mean values of the subtracted maps of patients 2, 5, 8, and 9 were 0.006 ± 0.003 (ranging from 0.000 to 0.014), 0.021 ± 0.015 (ranging from 0.000 to 0.056), 0.074 ± 0.045 (ranging from 0.000 to 0.140), and 0.044 ± 0.028 (ranging from 0.000 to 0.159) respectively. For all the patients, the maps were found to be statistically equivalent using the TOST analysis (p -value $\ll 10^{-6}$).

3.3 Impact of Referencing with Areola Tissue

STC spectra calculated with the contralateral areolar tissue as reference were obtained for the seven patients whose areolas were located in the field of view of the optical measurement. Similar STC spectra as the ones obtained using the contralateral breast as reference were obtained in four out of the seven patients, as shown in Fig. 4(a) for patient 4. We found an average correlation coefficient of 0.98 ± 0.01 (range 0.97 to 0.99) between the spectra referenced on the areola compared with the whole contralateral breast for these four patients. These spectra produced negligible differences in the STC index maps. The mean average (standard deviation, minimum–maximum) devi-

ations of the subtracted maps was 0.033 (ranging from 0.007 to 0.059) with an average SD of 0.0210 (ranging from 0.005 to 0.039). In three patients (Nos. 2, 9, and 11), the STC spectra calculated with the different referencing (i.e., contralateral areola vs. entire contralateral side) showed different spectral features, as shown Fig. 4(b) for patient 9. We found the following correlation coefficients: 0.56, 0.69, and 0.80, between the spectra referenced on the areola compared with the whole contralateral breast for patients 2, 9, and 11, respectively. In these patients with different STC spectra, we observe visually similar STC index maps, as shown by the subtracted maps in Fig. 5(a), 5(b), 5(d), 5(e), 5(g), and 5(h). The average deviations of the subtracted maps, in Fig. 5(c), 5(f), and 5(i) were 0.035 ± 0.023 (ranging from 0.000 to 0.101) and 0.034 ± 0.020 (ranging from 0.000 to 0.068) for these three patients. For all the patients, the maps were found to be statistically equivalent using the TOST analysis (p -value $\ll 10^{-6}$).

4 Discussion and Conclusion

The impact of reference selection is a critical issue for spectroscopic methods that utilize differential techniques for material characterization. In the case of *in vivo* tissue analysis, spatial variations in physiologic/biologic characteristics can potentially impact detection capability and reliability. In this study, we investigated both the number and location of reference measurements in order to determine their influence on the STC contrast function. Multiple regions within both the contralateral and ipsilateral breast were evaluated in 10 patients as reference sites for STC calculation and image formation.

Visual inspection and statistical results show that referencing on a few random points across the contralateral breast does not affect the STC spectra of the lesion, and subsequently do not affect the STC index maps in all 10 patients. The study included 5 premenopausal and 5 postmenopausal women, with various breast densities (3 BIRADS 4, 1 BIRADS 3, 3 BIRADS 2, and 3 unknown). This suggests that the STC approach is not dependent on the type of tissue, density, or on the heterogeneity of the breast used as reference. These results confirm that the main elements of tumor contrast were absent from normal breast tissue in the 10 patients. Normal tissue contains regions of vascularized fibroglandular tissue and fat, with different optical properties.²⁰ Therefore, our results also imply that the STC is not determined by the contrast in chromophore concentrations but by shifts in absorption spectral features. This is a potentially important result for the problem of detecting tumors in young women and individuals with mammographically dense breast tissue. With the SRDS method, discrimination between malignant and healthy glandular regions could be improved by focusing on shifts in the absorption spectra, due to the presence of specific tumor components.¹³

The selection of normal tissue reference locations from the ipsilateral (i.e., tumor-containing) side has also been investigated. STC spectra calculated using the contralateral and ipsilateral sides as reference was compared. Out of the 10 patients, 6 showed similar STC spectra in shape and magnitude, and 4 patients had differences in magnitudes or in shape within the spectral region 850 to 950 nm. Although these differences may reflect spectral heterogeneity of normal breast tissue, the

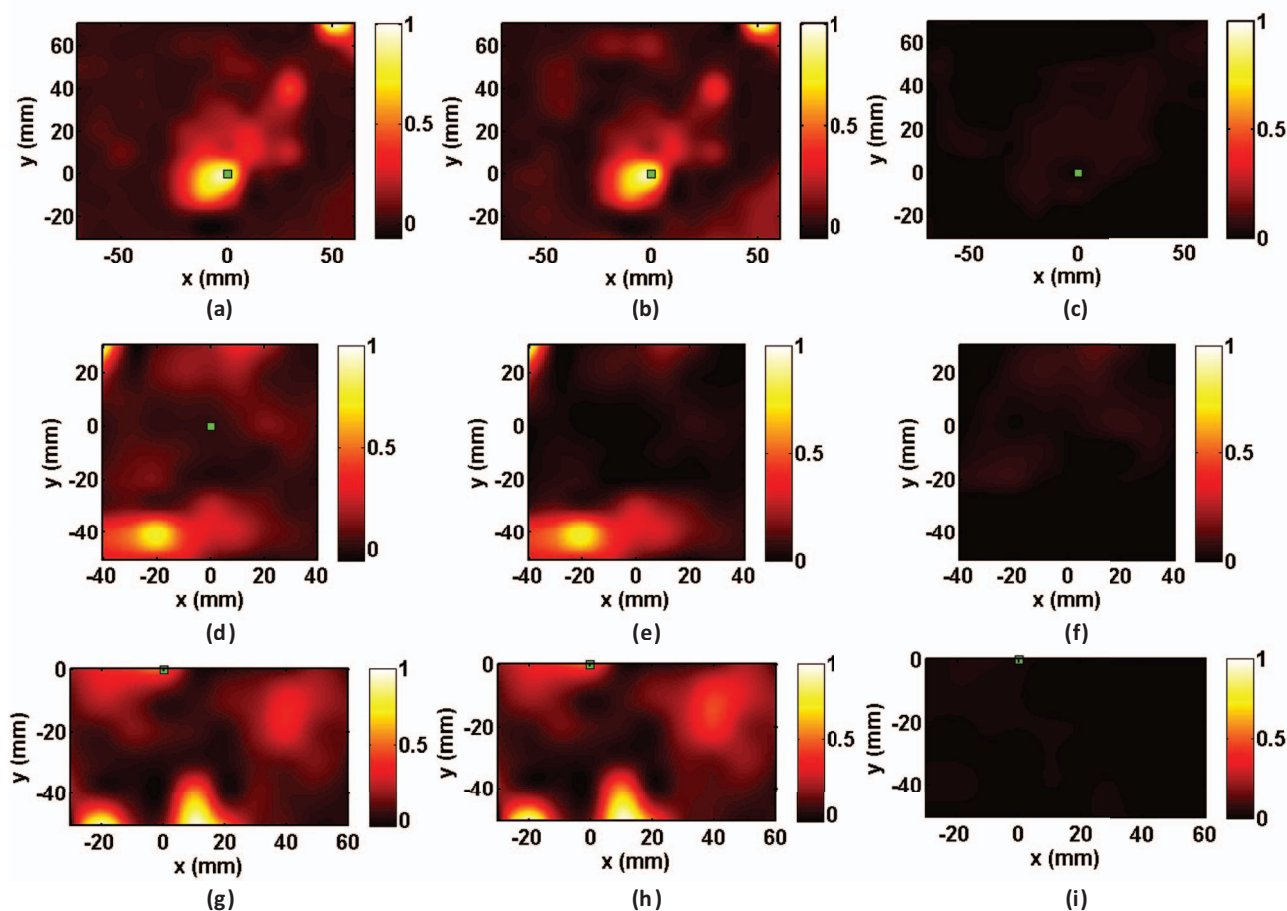


Fig. 5 (a) and (b) Normalized STC index maps of patient 2. (c) Subtracted map of patient 2. (d) and (e) Normalized STC index maps of patient 9. (f) Subtracted map of patient 9. (g) and (h) Normalized STC index maps of patient 11. (i) Subtracted map of patient 11. The STC index maps in (a), (d), and (g) are obtained using the contralateral breast as reference. The STC index maps in (b), (e), and (h) are obtained using the areola regions of the contralateral breast as reference.

origin of these signals is not precisely known. Recent studies have shown that malignant cancers alter lipid metabolism.^{21,22} As the main features are observed in the spectral region 850 to 950 nm, a reasonable hypothesis is that changes in hemoglobin, water, and lipid metabolism may be responsible for these differences observed in STC spectra. Nevertheless, the STC index maps of all the patients referenced on the ipsilateral side were very similar and statistically equivalent to the STC index maps referenced on the contralateral side. In one patient, a feature absent in the STC index map referenced on the contralateral breast was observed in the STC index map referenced on the normal tissue of the ipsilateral breast, as shown in Fig. 3(d) and 3(e). The origin of these features are not understood. Nevertheless, as in the other nine patients, the main features of the maps remained unchanged and the lesions were clearly visible using the two referencing approaches. This shows in the 10 patients that the referencing on the ipsilateral normal breast tissue does not impact lesion detectability.

The areola region was also tested as a reference location for the STC index in the seven patients with areolas in the field of view of the optical measurement. First, the STC spectra referenced on the areola contained unique spectral features. This suggests that the tumor biomarker was found in all lesions and

was not cancelled by referencing to the areola. Further, we observed in three patients that some spectral features were different in STC spectra referenced on the contralateral breast and on the areola. This could result from the introduction of a specific marker of areolas during the referencing. Using both referencing on the areola and on the contralateral side, we obtained visually similar and statistically equivalent STC index images for all the patients. Referencing on the areola seems therefore to minimally impact the imaging of the STC for lesion detection. This suggests that the STC index is based on spectral regions that are minimally influenced by the referencing on the areola and thus optimally chosen to specifically visualize the tumor signature.

The areola is the highest vascularized region of the breast. Optical images are often overwhelmed by the high contrast of areolas which may result in masking of areolar tumors. Because of the presence of muscle in the areolar region, additional components, such as myoglobin, may not be fully accounted for in spectral fits. The residual of the mismatch between areola tissue absorption and the four chromophore-spectra may thus be specific and unique to areola physiology. This would result in the existence of a spectral biomarker specific to this region and could explain STC features observed in areolas.

In one patient, the lesion was not visualized in the DOSI images. This patient was a premenopausal 48 year old woman with heterogeneously dense breasts. The lesion was located at 12 o'clock at 7 cm from the nipple according to the ultrasound report, which is the typical location for the glandular tree. The lesion might have thus been missed due to the high background noise from the glandular tissue.

A single patient with a DCIS was excluded from this analysis to maintain a more consistent population. This DCIS lesion was still visible in the STC images. However, the STC spectra of noninvasive carcinomas (such as DCIS) have not been characterized and thus comparison to the STC spectra of invasive carcinomas is premature.¹³ It is unknown whether the STC index as defined in this paper would be optimized to noninvasive carcinomas.

In this study, we investigated one patient with ILC. The lesion was visible in both the STC and STC index images. While the contrast in chromophore concentration values may be low in ILC, the STC signature may nevertheless be detected: the STC signature arises from changes in molecular disposition, not abundance. Previous studies have shown that we can observe two types of contrast using the STC: invasive malignant lesions versus normal tissue and invasive malignant lesions versus benign lesions.^{12,13} However, patients with ILC are not common and extensive analysis of the STC in ILC has thus not been achieved. It would be of interest to investigate a broader range of invasive and *in situ* diseases, such as ILC, DCIS, and LCIS, using SRDS/DOSI as they are often difficult to detect using common imaging modalities.

In conclusion, our preliminary findings from a 10 patient study show the STC approach is independent of the number and location of the normal reference points obtained from the contralateral side. This suggests that the STC is absent and independent from any type of breast tissue in the normal breast. In addition, we have shown that referencing on the ipsilateral breast preserved the information contained in the STC index maps as compared to the current referencing on the contralateral breast. Finally, referencing on the areolar region minimally impacts the STC index maps. In three patients, a presumed areolar biomarker seems to affect the STC spectra referenced on the areola. The results in the 10 patients suggest that any type of referencing does not affect lesion detectability, implying that the STC contrast is not contingent on the breast side, type, location, and amount of normal breast tissue. This confirms in the 10 patients the presence of NIR spectral components that are unique to cancer and absent from normal breast tissue.

Acknowledgments

This work was supported by the National Institutes of Health under Grant Nos. P41-RR01192 (Laser Microbeam and Medical Program: LAMMP), U54-CA105480 (Network for Translational Research in Optical Imaging: NTROI), U54-CA136400 (NTR), R01-CA142989, and P30-CA62203 (University of California, Irvine Cancer Center Support Grant). E.G. acknowledges the National Institutes of Health Laboratory for Fluorescence Dynamics Grant No. P41-RR03155. This project was supported by the American Recovery and Reinvestment Act of 2009. BLI programmatic support from the Beckman Foundation is acknowledged. Bruce J. Tromberg, Albert E. Cerussi,

and Enrico Gratton report patents, owned by the University of California, related to the technology and analysis methods described in this study. The DOSI instrumentation used in this study was constructed in a university laboratory using federal grant support (NIH). A Conflict of Interest disclosure has been reviewed by UC Irvine.

References

1. K. Suzuki, Y. Yamashita, K. Ohta, and B. Chance, "Quantitative measurement of optical-parameters in the breast using time-resolved spectroscopy - Phantom and preliminary *in-vivo* results," *Invest. Radiol.* **29**(4), 410–414 (1994).
2. B. J. Tromberg, N. Shah, R. Lanning, A. Cerussi, J. Espinoza, T. Pham, L. Svaasand, and J. Butler, "Noninvasive *in vivo* characterization of breast tumors using photon migration spectroscopy," *Neoplasia* **2**(1-2), 26–40 (2000).
3. V. Ntziachristos, A. G. Yodh, M. Schnall, and B. Chance, "Concurrent MRI and diffuse optical tomography of breast after indocyanine green enhancement," *Proc. Natl. Acad. Sci. U.S.A.* **97**(6), 2767–2772 (2000).
4. P. Taroni, G. Danesini, A. Torricelli, A. Pifferi, L. Spinelli, and R. Cubeddu, "Clinical trial of time-resolved scanning optical mammography at 4 wavelengths between 683 and 975 nm," *J. Biomed. Opt.* **9**(3), 464–473 (2004).
5. T. Yates, J. C. Hebden, A. Gibson, N. Everdell, S. R. Arridge, and M. Douek, "Optical tomography of the breast using a multi-channel time-resolved imager," *Phys. Med. Biol.* **50**(11), 2503–2517 (2005).
6. M. G. Pakalniskis, W. A. Wells, M. C. Schwab, H. M. Froehlich, S. Jiang, Z. Li, T. D. Tosteson, S. P. Poplack, P. A. Kaufman, B. W. Pogue, and K. D. Paulsen, "Tumor angiogenesis change estimated by using diffuse optical spectroscopic tomography: demonstrated correlation in women undergoing neoadjuvant chemotherapy for invasive breast cancer," *Radiology* **259**(2), 365–374 (2011).
7. D. Grosenick, K. T. Moesta, H. Wabnitz, J. Mucke, C. Stroszczynski, R. Macdonald, P. M. Schlag, and H. Rinneberg, "Time-domain optical mammography: initial clinical results on detection and characterization of breast tumors," *Appl. Opt.* **42**(16), 3170–3186 (2003).
8. P. Taroni, A. Torricelli, L. Spinelli, A. Pifferi, F. Arpaia, G. Danesini, and R. Cubeddu, "Time-resolved optical mammography between 637 and 985 nm: clinical study on the detection and identification of breast lesions," *Phys. Med. Biol.* **50**(11), 2469–2488 (2005).
9. Q. Zhu, E. B. Cronin, A. A. Currier, H. S. Vine, M. M. Huang, N. G. Chen, and C. Xu, "Benign versus malignant breast masses: Optical differentiation with US-guided optical imaging reconstruction," *Radiology* **237**(1), 57–66 (2005).
10. A. E. Cerussi, D. Jakubowski, N. Shah, F. Bevilacqua, R. Lanning, A. J. Berger, D. Hsiang, J. Butler, R. F. Holcombe, and B. J. Tromberg, "Spectroscopy enhances the information content of optical mammography," *J. Biomed. Opt.* **7**(1), 60–71 (2002).
11. X. Intes, "Time-domain optical mammography SoftScan: Initial results," *Acad. Radiol.* **12**(8), 934–947 (2005).
12. S. Kukreti, A. Cerussi, B. Tromberg, and E. Gratton, "Intrinsic tumor biomarkers revealed by novel double-differential spectroscopic analysis of near-infrared spectra," *J. Biomed. Opt.* **12**(2), 020509 (2007).
13. S. Kukreti, A. E. Cerussi, W. Tanamai, D. Hsiang, B. J. Tromberg, and E. Gratton, "Characterization of metabolic differences between benign and malignant tumors: high-spectral-resolution diffuse optical spectroscopy," *Radiology* **254**(1), 277–284 (2010).
14. T. H. Pham, O. Coquoz, J. B. Fishkin, E. Anderson, and B. J. Tromberg, "Broad bandwidth frequency domain instrument for quantitative tissue optical spectroscopy," *Rev. Sci. Instrum.* **71**(6), 2500–2513 (2000).
15. F. Bevilacqua, A. J. Berger, A. E. Cerussi, D. Jakubowski, and B. J. Tromberg, "Broadband absorption spectroscopy in turbid media by combined frequency-domain and steady-state methods," *Appl. Opt.* **39**(34), 6498–6507 (2000).
16. W. Tanamai, C. Chen, S. Siavoshi, and A. Cerussi, "Diffuse optical spectroscopy measurements of healing in breast tissue after core biopsy: case study," *J. Biomed. Opt.* **14**(1), 014024 (2009).

17. J. Rogers, K. Howard, and J. Vessey, "Using significance tests to evaluate equivalence between two experimental groups," *Psychol. Bull.* **113**(3), 553–565 (1993).
18. K. A. Garrett, "Use of statistical tests of equivalence (bioequivalence tests) in plant pathology," *Phytopathology* **87**(4), 372–374 (1997).
19. S. Wellek, *Testing Statistical Hypotheses of Equivalence*, London (2003).
20. N. Shah, A. Cerussi, C. Eker, J. Espinoza, J. Butler, J. Fishkin, R. Hornung, and B. Tromberg, "Noninvasive functional optical spectroscopy of human breast tissue," *Proc. Natl. Acad. Sci. U.S.A.* **98**(8), 4420–4425 (2001).
21. E. O. Aboagye and Z. M. Bhujwala, "Malignant transformation alters membrane choline phospholipid metabolism of human mammary epithelial cells," *Cancer Res.* **59**(1), 80–84 (1999).
22. M. Hilvo, C. Denkert, L. Lehtinen, B. Müller, S. Brockmüller, T. Seppänen-Laakso, J. Budczies, E. Bucher, L. Yetukuri, S. Castillo, E. Berg, H. Nygren, M. Sysi-Aho, J. L. Griffin, O. Fiehn, S. Loibl, C. Richter-Ehrenstein, C. Radke, T. Hyötyläinen, O. Kallioniemi, K. Iljin, and M. Orešič, "Novel theranostic opportunities offered by characterization of altered membrane lipid metabolism in breast cancer progression," *Cancer Res.* **71**(9), 3236–3245 (2011).